17th World Conference on Earthquake Engineering, 17WCEE
Sendai, Japan - September 13th to 18th 2020
Paper N° C003608
Registration Code: S-A01472

DYNAMIC ANALYSIS OF A HIGHWAY CUT AND COVER TUNNEL IN LIMA CITY, PERU

Z. Aguilar[(1)], L. Vergaray[(2)], J. Tarazona[(3)], J. Barrantes[(4)]

[(1)] *Principal Researcher, Peruvian-Japanese Center for Seismic Research and Disaster Mitigation, Peru, zaguilar@uni.edu.pe*
[(2)] *Research Assistant, School of Civil Engineering, National University of Engineering, Peru, lvegraraya@uni.edu.pe*
[(3)] *Research Assistant, School of Civil Engineering, National University of Engineering, Peru, jtarazonag@uni.edu.pe*
[(4)] *Research Assistant, School of Civil Engineering, National University of Engineering, Peru, jbarrantess@uni.edu.pe*

Abstract

In Peru, projects that involve underground structures being developed frequently in recent years, particularly in the city of Lima where a massive transportation network is developing. However, there is little local knowledge regarding the seismic analysis of these structures; furthermore, there are no Peruvian underground structures seismic design code available, which is recently being developed. Therefore, in this paper, to understand the seismic behavior of a "Cut and Cover Tunnel" in the gravel of the city of Lima, in this article, two approaches for the seismic analysis are presented. The first one considering a free field soil response analysis and the second one, a dynamic analysis of the cut and cover tunnel and soil interaction, for which strong ground motion time history records were obtained from a spectral matching process of past subduction earthquakes. 1D and 2D seismic site response analysis was performed using the finite element method and the HS Small constitutive model to modeling the dynamic behavior of soils, while the elastic model was employed on the reinforced concrete structures. The dynamic properties of the materials were estimated from geophysical tests and based on the literature for this type of gravelly alluvial soils. The seismic response analysis in terms of accelerations and displacements shows a strong influence of the presence of the cut and cover tunnel generates in areas close to the structure, besides, deformation patterns were observed on the lateral projections on the surface, highlighting the effects of the soil-structure interaction on the surrounding and surface soil.

Keywords: Underground structure seismic design, 'Cut and Cover' tunnel, soil-structure interaction

1. Introduction

The need for understanding the seismic behavior of buried structures and their interaction with the surrounding environment has greatly increased in Peru in recent years. As it is known, Peru is located in a highly seismic zone where seismic events of great intensity usually occur, which generate damage not only for buildings or other surface structures but also for newly buried structures that are being constructed in recent years. Furthermore, the lack of a Peruvian underground structures seismic design code, which is recently being developed, generates uncertainty on the seismic behavior of these kinds of structures, whose construction is underway.

Formerly, the seismic behavior of the tunnels was considered unimportant since it was assumed that their ability to withstand seismic demands was high due to soil confinement. It was not until considerable damage was observed in these types of structures, in Kanto (1923), Kobe (1995), and Chi-Chi (1999) earthquakes that the seismic behavior of underground structures cached the attention of many researchers around the world.

Currently, many investigations have been carried out regarding this topic under multiple approaches, being numerical modeling one of the favorite methods to evaluate the soil-structure interaction during an earthquake. The impact of the strong earthquake ground motion on the buried structures and their interaction with the surrounding soil is discussed in this article, using for this purpose the finite element method.

2. The geometry of the tunnel

The tunnel analyzed in the present research consists of a two-way rectangular structure, whose dimensions are presented in Fig. 1.

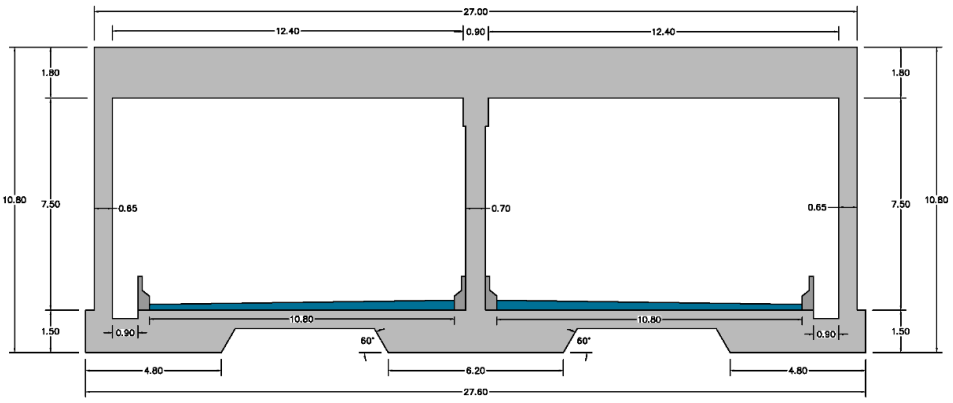

Fig. 1 – Geometry of the Tunnel.

The structural components were modeled by 'Plate' elements of linear elastic behavior formulated according to the Reissner-Mindlin theory [1]. Table 1 summarizes the parameters of the structural elements that have been adopted in the 2D model

Table 1 – Adopted parameters for the tunnel used in the model

Parameter	Unit	Upper beam	Lateral plates	Interior plate	External slab	Internal slab	Central slab
$E \times A$	kN/m	2.07E+07	1.80E+07	1.22E+07	3.09E+07	1.29E+07	4.38E+07
$E \times I$	kNm^2/m	5.35E+06	3.68E+05	1.43E+05	3.71E+06	2.68E+05	1.05E+07
δ	m	1.76	0.5	0.38	1.20	0.50	1.70
w	kN/m/m	19.0	16.5	11.2	28.3	11.8	40.0
α	-	0.02	0.02	0.02	0.02	0.02	0.02
β	-	0.02	0.02	0.02	0.02	0.02	0.02

3. Geotechnical Characterization

3.1 Geotechnical conditions of the study area

The city of Lima is located in the Plain of the Peruvian Coast, which represents one of the main geomorphological units that are distributed in the Peruvian territory. This unit covers a vast arid plain and, in Lima city, is crossed by the Chillón, Rimac, and Lurin Rivers. The study area is constituted by a deep deposit of alluvial soil that was dumped by the Rimac River on a depression now filled by boulders, gravels, sand, and clays of unknown thickness [2]. Fig. 2. (a) shows the Lima's gravel with particles bigger than the conventional 3" and cobbles, while in Fig. 2 (b) the particle size distribution.

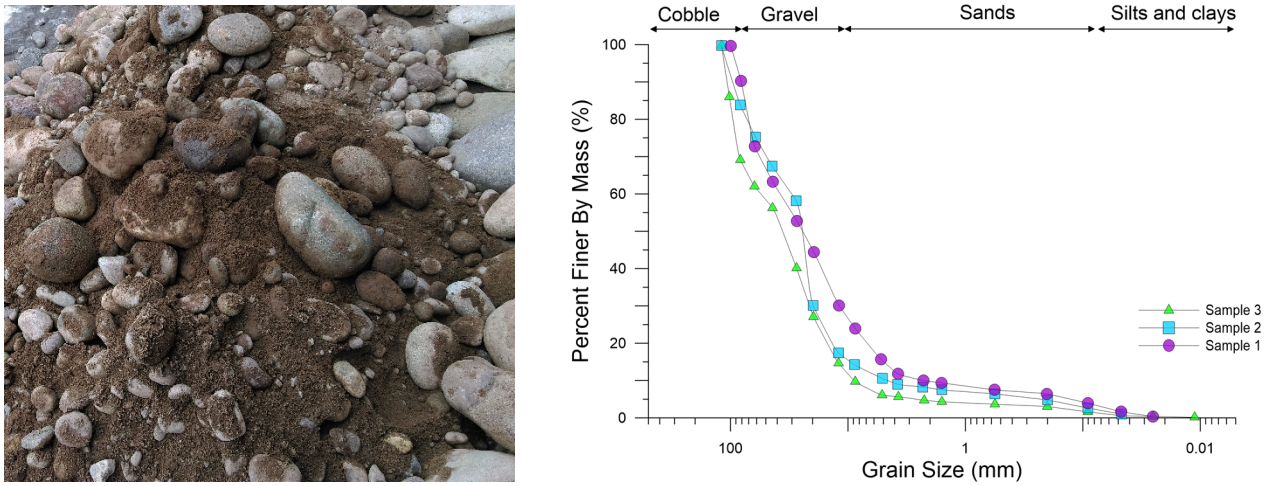

(a) (b)

Fig. 2 – (a) Photo of Limas' Gravel and (b) it particle size distribution.

Geophysical tests (i.e., MASW and MAM) were used to determine the elastic and dynamic characteristics of the soils, from which a representative Vs soil profile was obtained. Shear wave velocities higher than 800 m/s at depths larger than 40 meters show the presence of a very dense soil or rock, as shown in Fig. 3, which is characteristic of this soil deposit.

The shear strength parameters for each soil layer were chosen based on the bibliographic compilation of large-scale and in situ direct shear tests of Lima's gravel. [3]. Additionally, since there are no tests to determine the dynamic properties of the materials that conform the stratigraphic soil profile, the damping curves and shear modulus at small strains proposed by Menq [4] for granular soils have been used and compared with the other available relations in the literature (i.e., Rollins *et al*. [5], Lin *et al*. [6], Araei *et al*. [7]), showing a good correlation (Fig. 4).

3.2 HS-Small model fitting

In order to determine the effect a great magnitude earthquake could cause to underground structures in Lima, the gravel strata surrounding the tunnel have been modeled considering the HS-Small model since it is capable to developing the hysteretic elastic behavior of the soil at small strains in a more realistic way, introducing the initial shear modulus into the model formulation (G_0) and the reduction of the secant shear modulus to 70% to the initial G_0 ($G_{0.7}$), at a characteristic small strain ($\gamma_{0.7}$). [8]. The reference shear modulus (G_0^{ref}) was calculated indirectly using elastic relationships. Shear strain levels were defined around γ_0=1.00E-4. The values of the G_{ur}/G_0 ratio was assigned according to the depth, having higher values for the deeper strata. Based on the reference shear modulus G_0^{ref}, the G_{ur}/G_0 ratio of the materials, the defined Poisson values, and the loading and unloading elasticity modules were estimated according to Eur=Gur×2(1+νur).

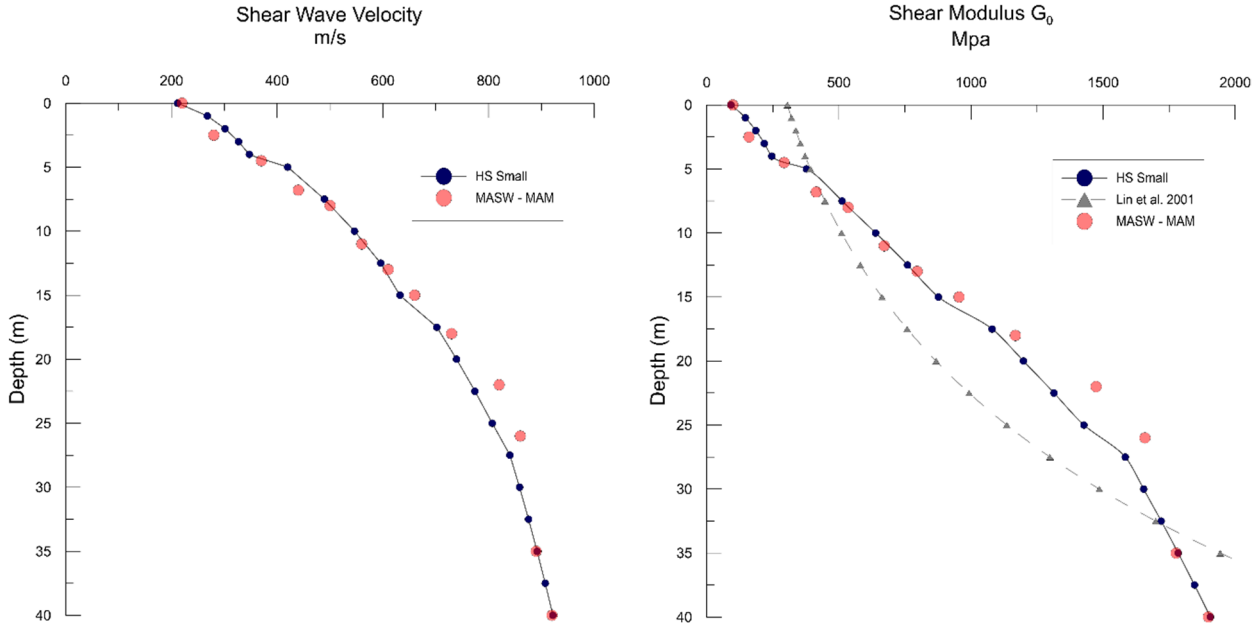

Fig. 3 – Shear wave velocity profile measured (red dots) and the calibrated (blue line) in the HS Small model.

For the parameters of the HS Small model, the axial load / reload stiffness value E_{ur}^{ref} has been assumed as three times the reference Young secant modulus E_{50}^{ref}. On the other hand, the reference oedometric module E_{oed}^{ref} has been considered equal to $[(K_0^{NC})/3]^{0.5}\ E_{ur}^{ref}$ [9].

The adjustment of the shear modulus at small strains has been carried out, considering the profile of shear wave velocity of the zone. On the left of Fig. 3, the comparison between the adjustment of the shear wave velocity profile of the calibrated HSS Model and the measured field profile is presented. Likewise, on the right side, the profile of the shear modulus from the geophysical tests, the profile adjusted for the HS Small model, additionally, the Lin *et al*. semi-empirical relationship [6] is presented. In both cases, a consistent fit of the model with the field measurements can be seen.

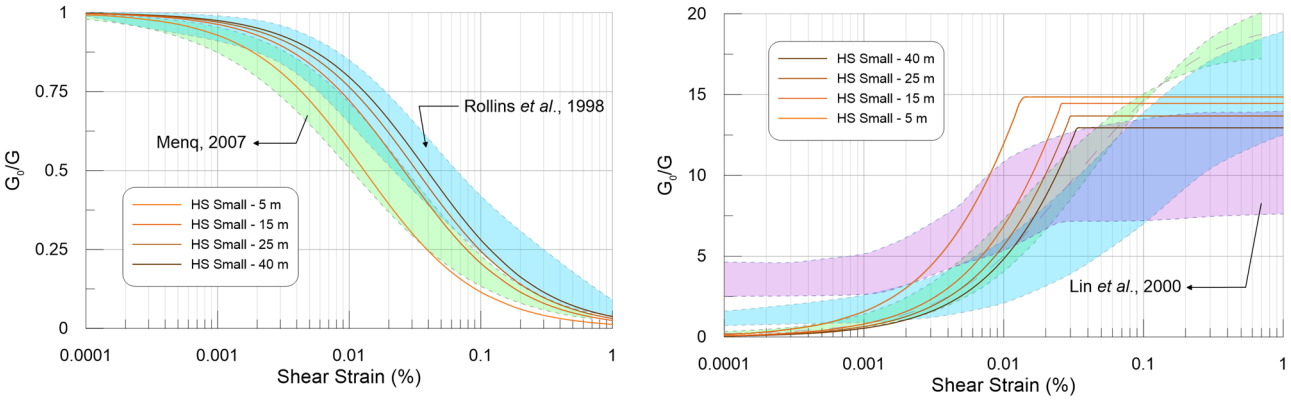

Fig. 4 - G/G_0 and Damping (%) vs shear strains (%)of the HS Small, left, and right, respectively.

Several recommendations in the literature can be used to define the Rayleigh coefficients [10], [11], [12]. However, the first control frequency has been taken as the natural frequency of the soil profile (f_s) and the second one as five times of that frequency [f_s *y* $5f_s$] based on Kwok *et al*.[12] and Sun & Dias [13].

Table 2 HS Small soil parameters considered in the modeling.

Parameter	Units	Depth			
		(0 – 4.5m)	(4.5 – 15m)	(15 – 26m)	(26 – 60m)
γ_{dry}	kN/m^3	2.04	2.14	2.19	2.24
γ_{wet}	kN/m^3	20	21	22	22
E_{50}^{ref}	kN/m^2	4.06E+04	1.32E+05	2.71E+05	3.96E+05
E_{oed}^{ref}	kN/m^2	2.54E+04	7.97E+04	1.57E+05	2.21E+05
E_{ur}^{ref}	kN/m^2	1.23E+05	4.00E+05	8.20E+05	1.20E+06
m	-	0.50	0.80	0.80	0.50
C	kN/m^2	10	10	20	20
ϕ	°	38	40	42	44
ψ	°	8	10	12	14
$\gamma_{0.7}$	%	7.50E-05	1.00E-04	1.25E-04	1.50E-04
G_0^{ref}	kN/m²	2.00E+05	6.50E+05	1.25E+06	1.75E+06
α	-	1.283	1.283	1.283	1.283
β	-	5.31E-04	5.31E-04	5.31E-04	5.31E-04

4. Seismic environment characterization

The seismogenic sources proposed by Aguilar *et al*. [14] were used to assess the seismic hazard at the site. There, the statistical analysis for the source characterization has been updated to 2018. The seismogenic sources that have influence in Lima city were determined within a circle of 400 km radius. Among the sources, three types of focal mechanisms were identified: interface, intraplate, and crustal ones. GMPE for each of them has been considered. Furthermore, in order to reduce the associated epistemic uncertainty, the use of a logical decision tree has been considered, which is shown in Table 3.

Table 3 - Weighting Values of the logical decision tree

GMPE		Interface	Intraplate	Crustal
		Weight		
BC Hydro (2016)	Δ C1 = Lower Values	0.2	-	-
	Δ C1 = Central Values	0.2	-	-
	Δ C1 = Upper Values	0.2	-	-
	Lower Value $\Delta C1 = -0.5$	-	0.2	-
	Central Value $\Delta C1 = -0.3$	-	0.2	-
	Upper Value $\Delta C1 = -0.1$	-	0.2	-
Zhao *et al*. (2006)		0.2	0.2	-
Youngs *et al*. (1997)		0.2	0.2	-
Atkinson & Boore (2014)		-	-	0.25
Chiou & Young (2014)		-	-	0.25
Abrahamson & Silva (2014)		-	-	0.25
Sadigh *et al*. (1997)		-	-	0.25

The cut and cover tunnel under analysis have been considered as an important structure based on the Peruvian Seismic Design Code E.030 (2019), which considers a 1000 years return period event for the design

earthquake. Thus, it is also consistent with the AASHTO (2017) specifications that consider a 7% probability of exceedance in 75 years of a lifetime for road structures.

Based on the seismic disaggregation, the dominant event in the study area was determined. It corresponds to subduction earthquakes with magnitudes Mw ≥ 7.0 at distances between 80 km and 140 km. Given the limited information on seismic records of these characteristics, interface earthquakes were used. Furthermore, Chilean earthquakes registered by the National Seismological Center (NSC) [15] were chosen to complement the small number of Peruvian records [16]. These records are shown in Table 4.

Table 4 – Earthquake records used in the Spectral matching process

Earthquake	Mechanism	Station	Date dd/mm/yy	Longitude (°)	Latitude (°)	Depth (km)	Magnitude (Mw)
Ancash 1970	Intraplaca	PQR	31/05/1970	-78.87	-9.36	64	7.8
Lima 1974	Interfase	PQR	03/10/1974	-77.98	-12.5	13	8.1
Atico 2001	Interfase	MOQ	23/06/2001	-73.77	-16.08	33	8.4
Valparaíso 1985	Interfase	UFSM	03/03/2018	-33.24	-72.04	33	8.0
Tarapacá 2005	Intraplaca	CUYA	13/06/2005	-69.13	-19.90	111	7.9
Maule 2010	Interfase	BO02	04/11/2016	-71.00	-35.06	95	6.4

The time-domain spectral matching process has been performed using the Seismo Match v. 2016 software [17]. The acceleration response spectra for 12 time-history records (6 earthquakes in 2 directions) were spectrally adjusted to a target uniform hazard spectrum of 7% in 75 years (Tr = 1000 years).

5. Numerical model

he 2016 PLAXIS software, which uses the finite element method, was used for the analysis [9]. A 2D geometry has been considered for analyzes in the free-field and soil-structure interaction conditions. The geometry of the model consists of a 200 m wide by 40 m thick section of ground (Fig. 5). The infinite half-space size was defined considering a length to width relationship W / H> 7 [18] having in the present case a W / H = 8 – 9.

The boundary conditions in the lateral sides are '*Free Field'* type, and a '*Compliant*' base has been considered. The finite elements discretization has been carried out with a total of 4617 triangular elements of 15 nodes, with an average size of 2.5 m, in order that the waves can propagate properly fulfilling the ratio $l \leq Vs_{min} / 8\ f_{max}$, where "l" is the maximum size of the element, $\lambda = V_s / f_{max}$ represents the wavelength of the highest frequency of the seismic input record and the lowest propagation velocity of the ground shear waves [19].

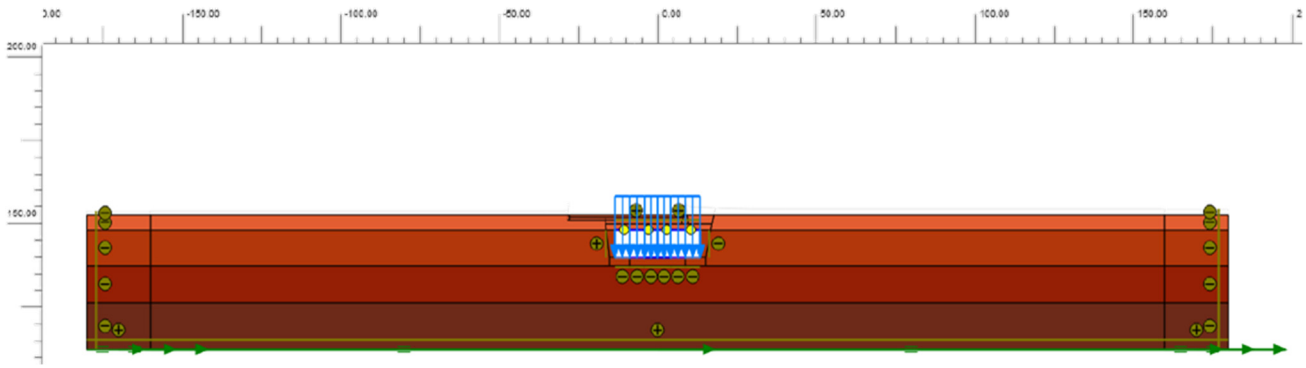

Fig. 5 – 2D FEM geometry model

The control points for accelerations and displacements are shown below in Fig. 6, so they are located at 0.00 m (A, E, H), 13.50 m (B, F, I), 27.00 m (C, G), and 40.50 m (D) meters from the tunnel external plate. These points are spaced at a distance equal to half the width of the tunnel. Additionally, a J point has been located at the base of the model to control the input ground motion.

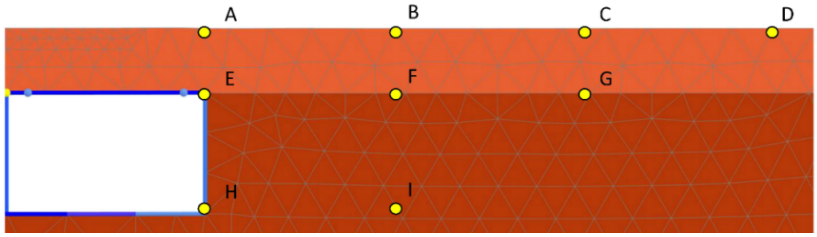

Fig. 6 – Control points at the surface (A-D), top (E-G), and bottom (H, I) of the tunnel.

6. Results and discussion

A series of dynamic analyses were carried out with the two-dimensional model, considering 06 seismic events in 2 directions. It is a fact that the inclusion of structures buried in a medium modifies the seismic response of the site. An interesting question is how the addition of a structure is going to affect the response of the soil. Here, there are a large number of factors that control this behavior, starting from the site condition, the structure and ground rigidity relationship, the nonlinearity of soil, the characteristics of earthquakes used for the analysis in terms of intensity and duration, among many others.

6.1 Vertical Displacements

Fig. 7 shows the typical behavior of vertical displacements when the EW Ancash earthquake is used. This behavior occurs in all the analyzes with variations in the settlement magnitude. Although the input movement is horizontal and the models have a completely flat topography, considerable displacements can be generated in the vertical direction, possibly due to the way the seismic waves are reflected and refracted in the tunnel walls.

The lifting effect, although smaller in magnitude compared to settlements in the lateral areas, is closely related to the depth at which the tunnel is buried, and this effect will gradually decrease as the tunnel location becomes deeper [20]. In the lateral sides of the tunnel, an order of -10 cm settlement is generated, while in the central area of the tunnel, slight uprisings up to 0.2 cm occur.

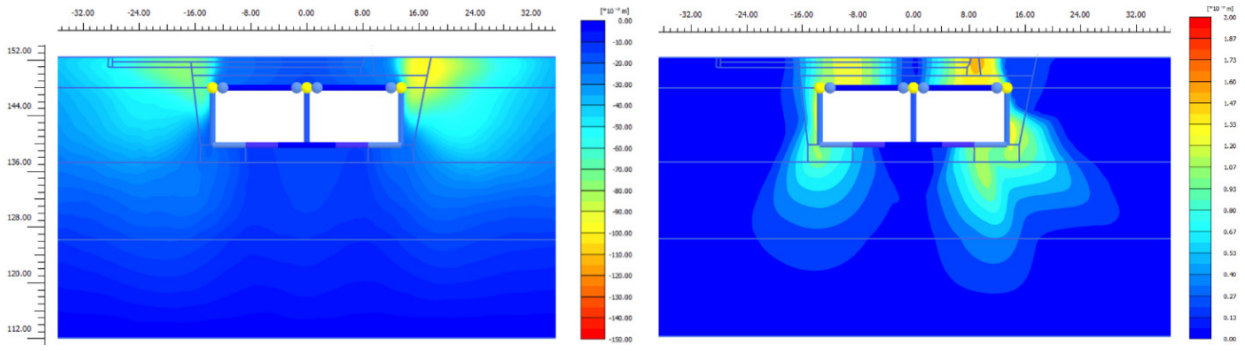

Fig. 7 – Maximum vertical displacement in the positive direction (left) and negative (right)

6.2 Shear Strain in the soil

To understand the way in which the deformations are attenuated and accentuated, it would be appropriate to review those areas where the ground reaches more significant strains, as well as the patterns under which these increments occur. In order to appreciate it, Fig. 8 shows a typical case of the maximum shear

deformations generated in the soil surrounding the tunnel under the EW Lima earthquake. The maximum values of shear strains occur in the lateral boundary of the top of the tunnel, forming a sort of arch towards the surface and cones towards the lateral ones with much less intensity.

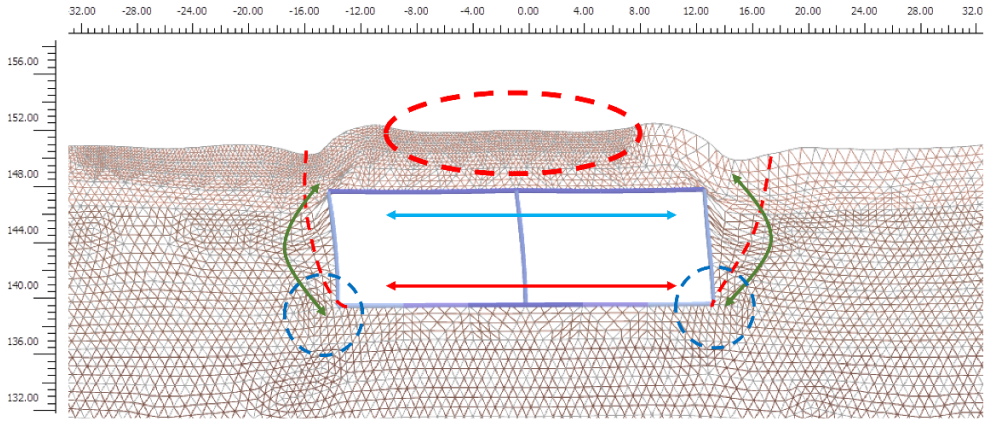

Fig. 8. Shear deformation pattern.

The pattern that shear strains are distributed on the lateral edges of the tunnel is related to how the tunnel deforms, the "Racking" type deformation, since the maximum shear deformations occur in the roof, where the maximum distortions of the structure occur. This distribution is similar in each of the analyzed cases, varying only in the magnitude of the results.

In addition, observing the lateral walls of the tunnel and its projection on the surface, significant strains were generated, tending to a volume reduction because the HS Small model is capable of reproducing the coupled behavior of the ground, creating volumetric strains due to the generation of shear stress. Therefore, it explains the fit observed in the shapes of the areas of Fig. 9 (left part) and those areas of considerable shear deformation.

The shear and volumetric deformations generated by an earthquake can be interpreted as a result of the “Racking” movement during the randomly shaking of the earthquake, which tends to exert forces contrary to the ground movement and increment the deformations that occur in the soil on the areas surrounding the tunnel. The development of these deformations is also intrinsically related to the non-linear behavior of the ground, and therefore to the development of residual and internal forces [21].

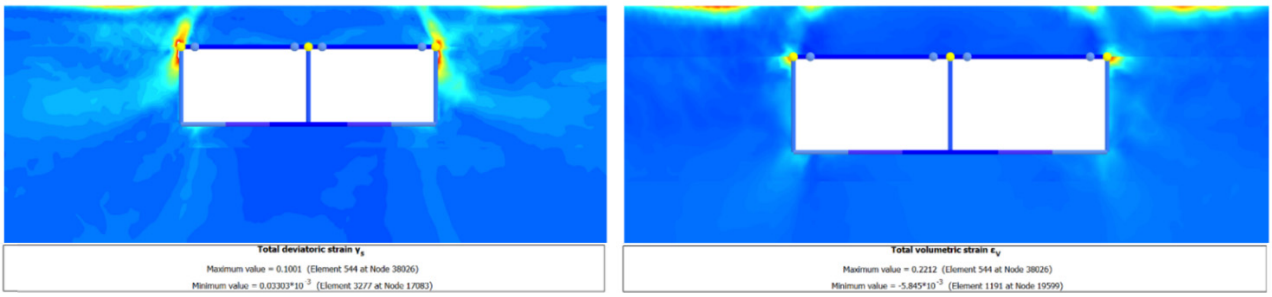

Fig. 9 – Distribution of shear strains γ_s and volumetric strains ε_v in the vicinity of the tunnel, respectively.

6.3 Soil degradation

To verify the relationship between the ground deformations and the nonlinearity of soil, the hysteresis loops for the free field condition (left side) and when the tunnel is buried (right side) are presented in Fig. 10. There, the color scale is presented as a function of time. It can be noted that broader hysteresis loops are developed at points A, B, E, and I, which show a more significant nonlinearity behavior of the soil. In turn, it demonstrates that after the earthquake, residual deformations in the ground occur. On the other hand, C, D, F, and G points

do not show much variation; therefore, the increment in the non-linearity of soils depends not only on the distance but also in the relative position from the tunnel.

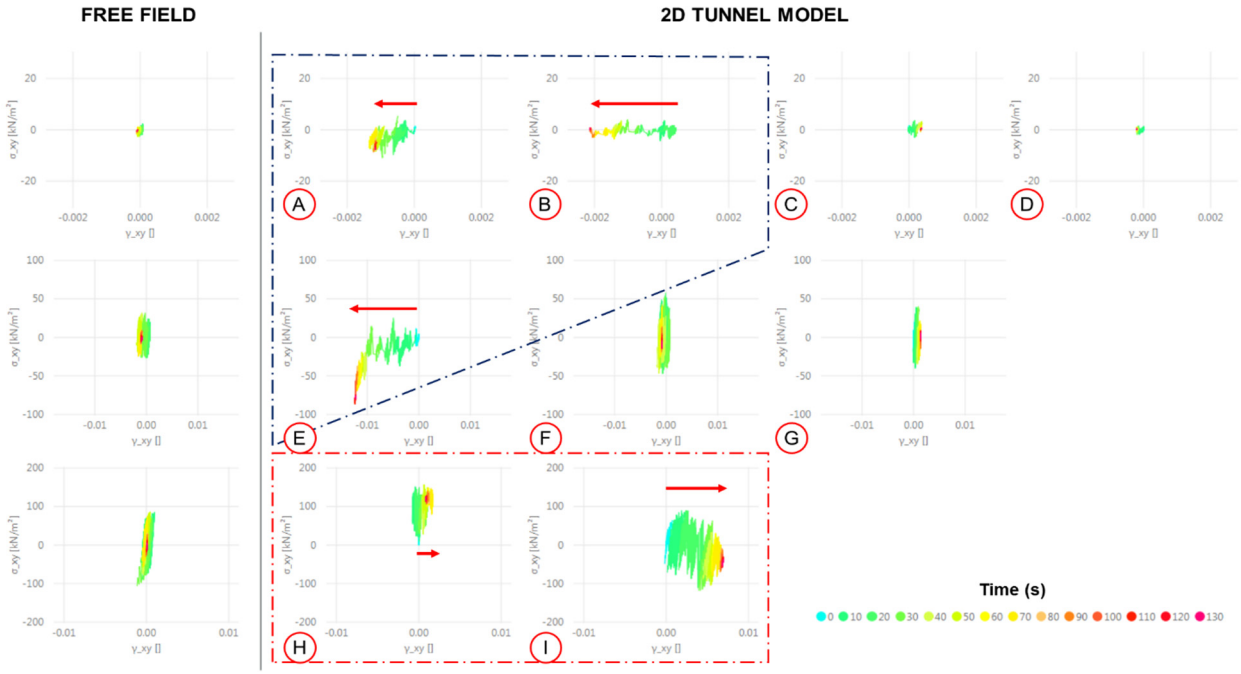

Fig. 10 – Hysteresis loops for the Maule EW Earthquake

6.4 Acceleration response spectrum

When comparing the results of the analyses for free-field condition and tunnel interaction models, it can be seen that the second one generates a significant increase in the seismic accelerations on the ground surface. In order to visualize it, the results of the A, B, C, and D control points will be analyzed Fig. 11 These increases in accelerations and displacements in the movement of the terrain are because the tunnel turns out to be more flexible than the ground itself, allowing more significant lateral displacements; this behavior naturally evidenced by other authors. [22].

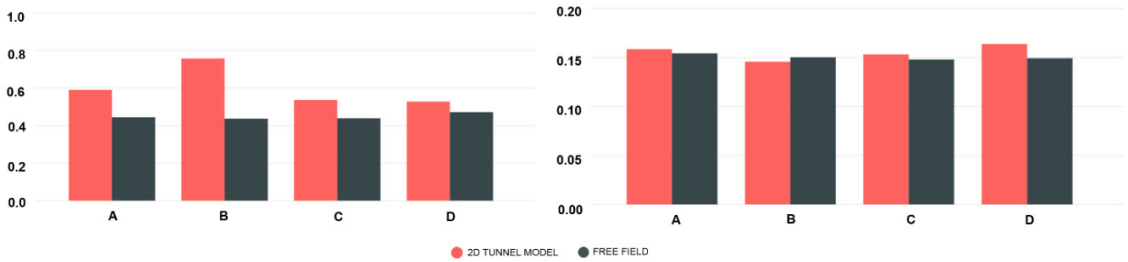

(a) (b)

Fig. 11 – Averages of maximum surface (a) acceleration in g and (b) displacements in m.

The increases in accelerations and displacements of the ground surface movement are because the tunnel turns out to be more flexible than the ground itself, allowing more significant lateral displacements; this behavior naturally was evidenced by other authors. [22]. Additionally, the comparison of the response spectra for free-field conditions and tunnel interaction has been made. Fig. 12 shows the averages of the acceleration spectrum at the surface control points. As expected, the seismic response of the ground is significantly affected in the vicinity of the tunnel, generating an amplification of the accelerations at the PGA level and other short periods (T = 0.10 s) levels, as well as attenuation for periods between 0.20 and 0.50 s. Moreover, this influence is attenuated as the distance from the tunnel increases.

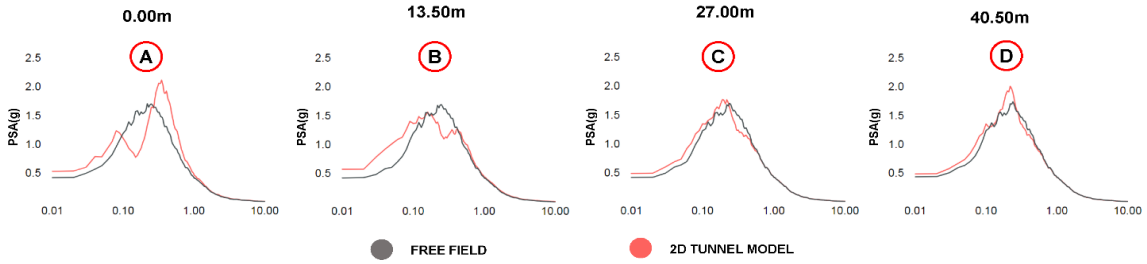

Fig. 12 – Comparison of the acceleration response spectrum.

The change in the seismic acceleration response is also reflected in the displacement spectrum, Fig. 13 shows the average of the horizontal displacement response spectra for the analyzed cases. It should be noted that, although in short periods, there is no significant variation in seismic behavior, in long periods, there is an amplification in displacements. As in the acceleration spectrum, this effect decreases as the distance from the tunnel increases.

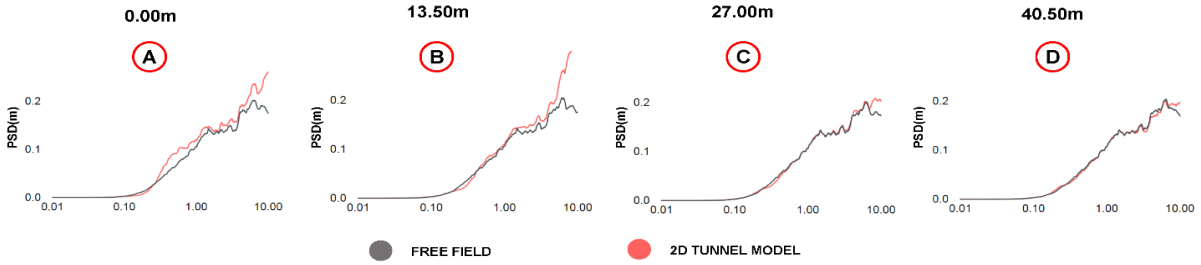

Fig. 13 – Comparison of the displacement response spectrum.

The amplification ratio of the tunnel interaction and free field models are shown in Fig. 14. The solid line represents the average of the results and the broken lines, the standard deviations. Although erratically, a seismic amplification at short and long periods is more noticeable, being consistent with that indicated in the accelerations and displacements spectra. In addition, there is a range between 0.20 and 0.50 s in which the response is not affected.

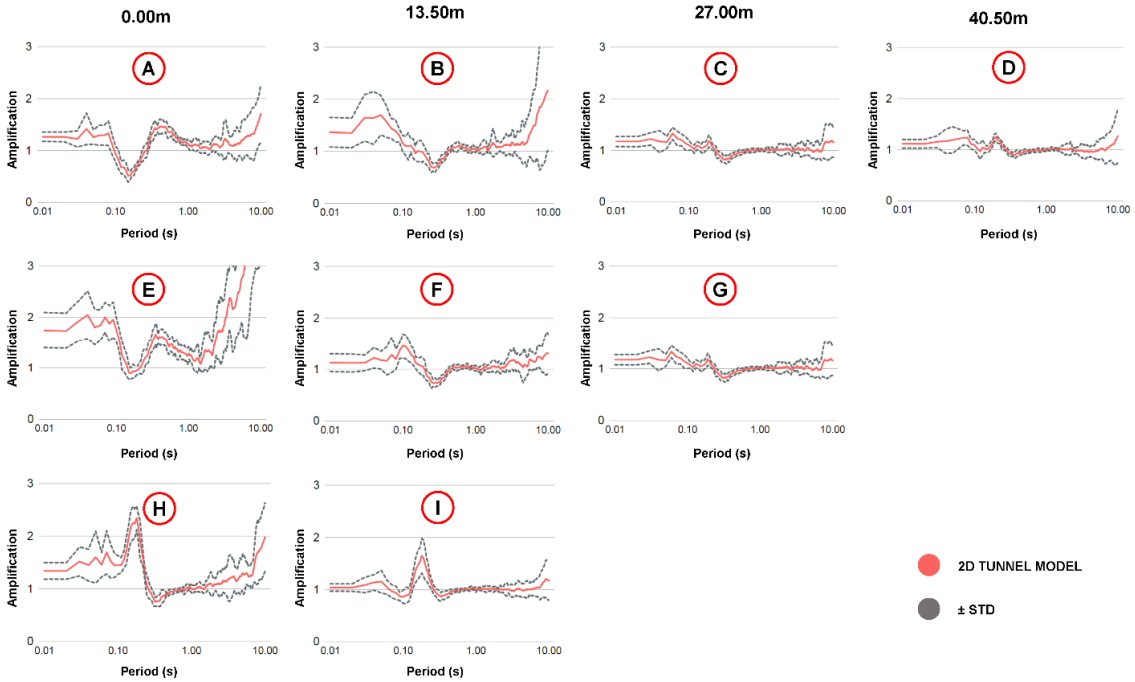

Fig. 14 – Amplification factor for Free Field and Interaction model.

In both terms, accelerations, and displacements, there is a change in the seismic response of the ground surface, (A, B, C, and D Points), the level of the upper beam (E, F, G) and at the bottom of the tunnel (H, I). Although it may seem a minor effect, accelerations can significantly alter the response of conventional buildings that are superficially grounded, such as high-rise buildings whose design is governed by the displacements of the ground.

Additionally, with the sole purpose of demonstrating the disadvantages of the analyzes in the free-field condition, a single additional analysis considering structural elements has been included. Comparing the condition with surface structures with the flat surface model shows a more significant distortion in the model, which implies a modification in the deformation patterns of the tunnel walls (Fig. 15).

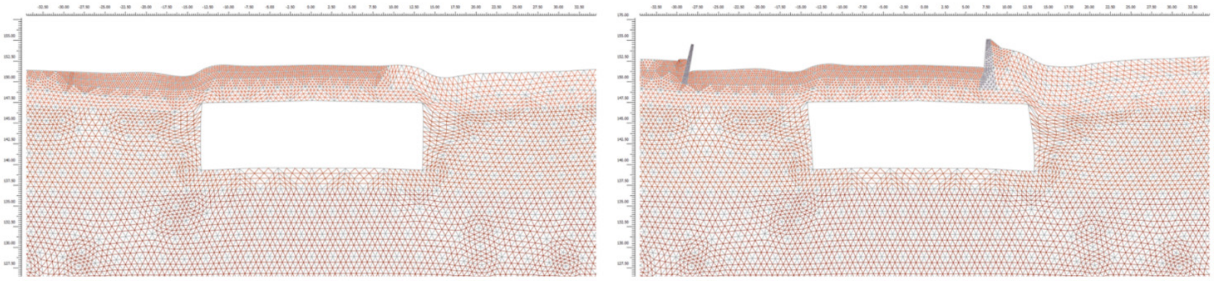

Fig. 15 –Residual displacements Ancash EW Earthquake, magnified 25 times.

This demonstrates that simplified methods such as unidimensional free-field analysis have certain limitations because they focus only on the analysis of tunnel displacements given their interaction with the soil, ignoring any consideration of the influence that other structures or topographical accidents could exert from the study site towards the tunnel. In densely populated urban areas, tunnels and other underground structures often pass under high-rise buildings or are located near them. The existence of these structures can create complex effects of interaction with underground structures, recently called "City effects "[21].

Finally, it can be said that this variability in the results allows knowing multiple ways in which the surrounding areas are influenced by the location of some underground structure, which becomes important because it modifies the response of the ground surface on which other structures were found. Therefore, this behavior should be taken into account for the seismic design of these surface structures.

7. Conclusions

The soil structure interaction of a cut and cover tunnel has been analyzed. The geometry of the tunnel has been defined, and the geotechnical characterization of the study area was performed. The results show the occurrence of considerable displacements in the vertical direction, despite the flat topography of the model, and the seismic waves entered at the base were horizontal. Besides, the maximum deformations in the soil surrounding the tunnel occur at the lateral limits of the upper level and in the areas close to the sidewalls of the tunnel and its projection on the surface.

Furthermore, the presence of a buried structure will increase nonlinearity in soil behavior, which in turn would indicate the existence of permanent deformations in the soil. The interaction of the tunnel with the surrounding soil during a seismic event generates an increase in seismic accelerations and displacements in the ground surface significantly. Also, the seismic response of the ground is significantly affected in the vicinity of the tunnel, generating an increase and attenuation in accelerations. This influence is attenuated as the distance to the tunnel increases.

To conclude, the existence of a buried structure, such as the ‘Cut and Cover’ tunnel of this research, has a significant impact by modifying the seismic response of the surrounding terrain within a certain range, this modification in the soil response during earthquakes should be considered as important as the response of the tunnels because this can affect other city infrastructure, especially in urban areas.

8. References

[1] Bathe, K. J. (1982). Finite Element Analysis in engineering analysis. *New Jersey: Prentice-Hall*.

[2] CISMID. (2015): Microzonificación Sísmica del Distrito Del Rímac. *Universidad Nacional de Ingeniería, Facultad de Ingeniería Civil*, Lima, Perú.

[3] Sánchez, S., & Rodríguez, J. (2016): Caracterización de suelos granulares gruesos. El caso de la Grava de Lima. *Simposio Nacional de Ingeniería Geotécnica y 5ª Jornadas Luso-Españolas de Geotecnia,* pp. 305-312, La Coruña, España.

[4] Menq, F. H. (2003): Dynamic Properties of Sandy and Gravelly Soils. Ph.D. Dissertation, *University of Texas at Austin,* United States of America.

[5] Rollins, K., Evans, M., Diehl, N., & Daily, W. (1998): Shear modulus and damping relationships for gravels. *Journal of Geotechnical and Geoenvironmental Engineering Vol 125, Issue 5, 398–405.*

[6] Lin, S.-Y., Lin, P. S., Hong-Su, L., & Juang, C. H. (2000): Shear modulus and damping ratio characteristics of gravelly deposits. *Canadian Geotechnical Journal, Vol 37, 638-651*.

[7] Araei, A. A., Razeghi1, H., Tabatabaei, S., & Ghalandarzadeh, A. (2010): Dynamic Properties of Gravelly Materials. *Scientia Iranica, 17(4), 245-261*.

[8] Benz, T. (2006): Small-Strain Stiffness of Soils and its Numerical Consequences. *Universität Stuttgart, Inst. für Geotechnik*, Germany.

[9] Brinkgreve, R. B. J., Kumarwamy, S., & Swolfs, W. M. (2016):.Plaxis 2016 Material Models Manual pp 65-92, Netherlands.

[10] Hudson, M., Idriss, M., & Beirkae, M. (1994). QUAD4M User's manual.

[11] Hashash, Y. P. (2010). Recent Advances in Non-Linear Site Response Analysis. *Fifth International Conference on Recent Advances in Geotechnical Earthquake Engineering and Soil Dynamics, Paper no. OSP 4.*

[12] Kwok, A. O., Stewart, J. P., Hashash, Y. M., Matasovic, N., Pyke, R., Wang, Z., & Yang, Z. (2007). Use of Exact Solutions of Wave Propagation Problems to Guide Implementation of Nonlinear Seismic Ground Response Analysis Procedures. *Journal of Geotechnical and Geoenvironmental Engineering, 1385–1398.*

[13] Sun, Q., & Dias, D. (2018). Significance of Rayleigh damping in nonlinear numerical seismic analysis of tunnels. Soil Dynamics and Earthquake Engineering, 115, 489–494. doi:doi:10.1016/j.soildyn.2018.09.013

[14] Aguilar, Z., & Vergaray, L. (2018). Superficie de subducción para los cálculos de peligro sísmico en el Perú. *XX Congreso Nacional de Ingeniería Civil.* Lima.

[15] Universidad de Chile: Centro Sismológico Nacional (CSN), http://www.sismologia.cl/

[16] CISMID: Red de acelerógrafos del CISMID/FIC/UNI, http://ceois.cismid-uni.org/red/

[17] Seismosoft (2016) "*SeismoMatch 2016* – A computer program for spectrum matching of earthquake records" available from http://www.seismosoft.com.

[18] Lilhanand, K., & Tseng, W. (1987). Generation of synthetic time histories compatible with multiple-damping design response spectra. *Transactions of the 9th International Conference on Structural Mechanics in Reactor Technology, 105-110.*

[19] Kuhlemeyer, R., & Lysmer, J. (1973). Finite element method accuracy for wave propagation problems. Journal of Soil Mechanics and Foundations Division, 421-427.

[20] Cheng, X., & Sun, Z. (2018). Effects of Burial Depth on the Seismic Response of Subway Station Structure Embedded in Saturated Soft Soil. *Hindawi Advances in Civil Engineering Volume 2018, 1-12.*

[21] Pitilakis, K., & Tsinidis, G. (2014). Performance and Seismic Design of Underground Structures. *In M. Maugeri, & C. Soccodato (Eds.). Earthquake Geotechnical Engineering Design (Vol. 28, pp. 279-340)*. Istambul, Turkey.

[22] Hashash, Y. M., Hook, J. J., Schmidt, B., & Chiang Yao, J. I. (2001). Seismic design and analysis of underground structures. *Tunneling and Underground Space Technology, 247-293*.